Characterizing x-ray transmission through filters used in high energy density physics diagnostics

J. Pearcy, N. Kabadi, A. Birkel, P. Adrian, B. Lahmann, B. Reichelt, T. M. Johnson, G. Sutcliffe, J. Kunimune, M. Gatu-Johnson, A. Bose, and C. K. Li

COLLECTIONS

Paper published as part of the special topic on Proceedings of the 23rd Topical Conference on High-Temperature Plasma Diagnostics

View Online   Export Citation   CrossMark

ARTICLES YOU MAY BE INTERESTED IN

Cell-phone camera Raman spectrometer
Review of Scientific Instruments **92**, 054101 (2021); https://doi.org/10.1063/5.0046281
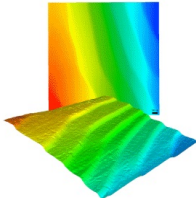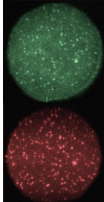
Development of a fast response neutron detector for the supersonic FRC collision process
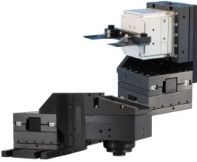Review of Scientific Instruments **92**, 063501 (2021); https://doi.org/10.1063/5.0043609

High-repetition rate solid target delivery system for PW-class laser–matter interaction at ELI Beamlines
Review of Scientific Instruments **92**, 063504 (2021); https://doi.org/10.1063/5.0053281

Nanopositioning Systems   Modular Motion Control   AFM and NSOM Instruments   Single Molecule Microscopes

MCL
MAD CITY LABS INC.
www.madcitylabs.com

Characterizing x-ray transmission through filters used in high energy density physics diagnostics

J. Pearcy,[a] N. Kabadi, A. Birkel, P. Adrian, B. Lahmann, B. Reichelt, T. M. Johnson, G. Sutcliffe,
J. Kunimune, M. Gatu-Johnson, A. Bose, and C. K. Li

AFFILIATIONS

Massachusetts Institute of Technology, Plasma Science and Fusion Center, Cambridge, Massachusetts 02139, USA

Note: Paper published as part of the Special Topic on Proceedings of the 23rd Topical Conference
on High-Temperature Plasma Diagnostics.
[a]Author to whom correspondence should be addressed: pearcy@mit.edu

ABSTRACT

We report on the design and implementation of a new system used to characterize the energy-dependent x-ray transmission curve, $\Theta(E)$, through filters used in high-energy density physics diagnostics. Using an Amptek X-123-CdTe x-ray spectrometer together with a partially depleted silicon surface barrier detector, both the energy spectrum and total emission of an x-ray source have been accurately measured. By coupling these detectors with a custom PROTO-XRD x-ray source with interchangeable cathodes, accurate characterizations of $\Theta(E)$ for filters of varying materials and thicknesses have been obtained. The validity of the technique has been confirmed by accurately reproducing areal densities for high-purity filters with known x-ray transmission properties. In this paper, the experimental setup is described and the results of absorption calibrations performed on a variety of different filters are presented.

Published under an exclusive license by AIP Publishing. https://doi.org/10.1063/5.0043770

I. BACKGROUND AND MOTIVATION

X-ray diagnostics of various kinds are critical to the study of high-energy density physics (HEDP), where they are employed at many institutions for a wide array of purposes. For example, x-ray diagnostics at the OMEGA Laser Facility include the Cryo Particle X-ray Temporal Diagnostic (CryoPXTD) used for the measurement of time-resolved electron temperature,[1] the x-ray penumbral imager for measuring electron temperature profiles,[2] and the Rowland x-ray spectrometer (XRS),[3] and at the National Ignition Facility, the Titanium Differential Filter Spectrometer (TiDFS)[4] for measuring the hotspot temperature and the Streaked Polar Instrumentation for Diagnosing Energetic Radiation (SPIDER).[5]

All these diagnostics involve some form of x-ray filtration, wherein the x rays are incident on a filter with certain transmission properties before being measured. Thus, the characterization of the filters used in these diagnostics is critical for the interpretation of their data. If the filters were constructed with ideal material properties, then their x-ray attenuation could be accurately inferred from their physical thicknesses using the tabulated data.[6] The tabulated mass attenuation coefficients are calculated from the theoretical total

cross sections for photon interactions—for information about the specific theoretical model used, see Ref. 6. However, elemental impurities within the filters can significantly alter their x-ray transmission rates and are more difficult to quantify than filter thicknesses. Therefore, it is valuable to be able to measure the x-ray transmission of such filters directly.

II. MEASURING TRANSMISSION CURVES

The degree to which x rays are attenuated in a material is dependent on the energy of the incident photon E. The object we refer to as a "transmission curve," or $\Theta(E)$, is the x-ray transmission of a given filter as a function of the photon energy.

In principle, measuring $\Theta(E)$ is quite straightforward. Given an x-ray source that is constant in time, one can measure the x-ray energy spectrum from the source in the absence of any filter $S_u(E)$ and the spectrum of the same source with the filter inserted between the source and spectrometer $S_f(E)$. Then, these spectra must be normalized to the total x-ray emission of the source during the exposures. If the total x-ray emission during the unfiltered measurement is A_u and the total emission during the filtered source

is A_f, the transmission curve is given by the expression

$$\Theta(E) = \frac{A_u}{A_f} \frac{S_f}{S_u}. \qquad (1)$$

If the x-ray source is constant in time, we are free to take $A_{u,f} = \tau_{u,f}$, where τ_u and τ_f are the exposure times of the unfiltered and filtered measurements, respectively (this subscript convention will be used throughout the remainder of this report). However, if the time-dependence of the source is unknown or poorly characterized, the exposure time is no longer a sensible proxy for $A_{u,f}$ and these normalization constants must be measured alongside the spectra themselves for a proper normalization to be performed. In general, the fluence from the source is a function of time $C(t)$. By measuring the fluence, one can calculate the true normalization coefficients,

$$A_{u,f} = \int_{t_{u,f}}^{T_{u,f}} C(t) \ dt, \qquad (2)$$

where $t_{u,f}$ and $T_{u,f}$ are the start- and end-times for the respective exposures. Therefore, by measuring the quantities $S_{u,f}$ and $C(t)$, the transmission curve $\Theta(E)$ may be directly calculated.

III. DIAGNOSTIC DESIGN

In order to realize these measurements, an "x-ray test bench" for characterizing diagnostic filters was designed.

A schematic and a photograph of the x-ray test bench setup are shown in Figs. 1 and 2. An AMPTEK X-123-cdte x-ray spectrometer[7] was used to measure spectra $S(E)$ alongside a partially depleted silicon surface barrier detector (SBD)[8] connected to an electrometer to measure $C(t)$. The SBD is a p–n type silicon diode wafer with a thin depletion layer; for more information about the SBD itself, see the documentation available in Ref. 7. Using this setup
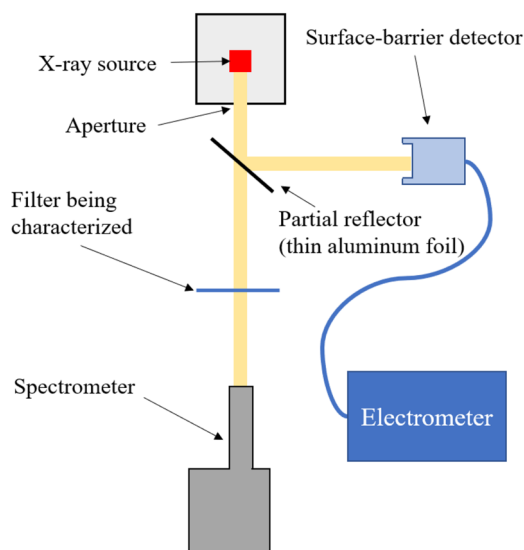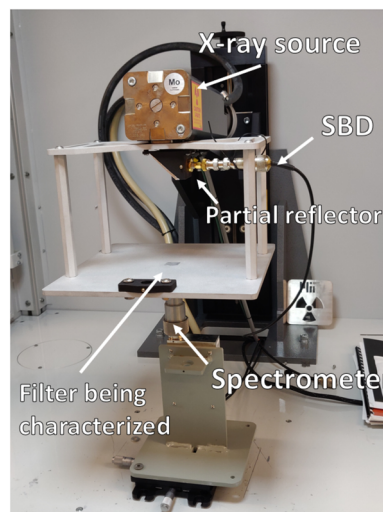

FIG. 2. A photograph of the x-ray test bench setup with relevant componenets labeled.

together with a custom PROTO-XRD x-ray source, accurate measurements of $\Theta(E)$ for filters of various materials over a wide range of energies have been obtained.

X rays from the source stream out through an aperture toward the spectrometer. Along the way, some fraction of the photons are scattered incoherently off of a thin aluminum foil (acting as a partial reflector) into the SBD, providing a measurement of $C(t)$. The stream of photons that passes through the partial reflector is then attenuated by the filter being measured before being collected in the spectrometer, providing a measurement of $S(E)$.

A system design that does not include the use of a partial reflector is possible, and would result in higher count rates observed by the spectrometer—however, the SBD is sensitive to visible light and therefore requires shielding. In this setup, the partial reflector serves a dual purpose, doubling as both a shield from visible light and blocking the direct line of sight between the filter being characterized and the SBD. This is important as it prevents x rays scattered off the foil being characterized from affecting the C(t) measurement.

IV. DEMONSTRATION OF SYSTEM CAPABILITIES

A. Unfiltered emission from the x-ray source

The Proto-XRD source can be fitted with a number of different anode tubes, each of which has a different x-ray spectrum. This allows the user to select a tube that has spectral peaks in an energy region of interest, providing better statistics in that energy region for a given exposure time.

Currently, the test bench is equipped with tubes made of copper, molybdenum, and titanium. The unfiltered spectra for these three tubes are shown in Fig. 3. For example, it can be seen that the copper tube is ideal for calculating transmission curves for incident photons energies below 10 keV, while the molybdenum tube is better suited to calculating transmission curves in the 10–20 keV region.

FIG. 1. A schematic diagram of the x-ray test bench setup with relevant components labeled. The x rays are schematically represented by the pale yellow beam.
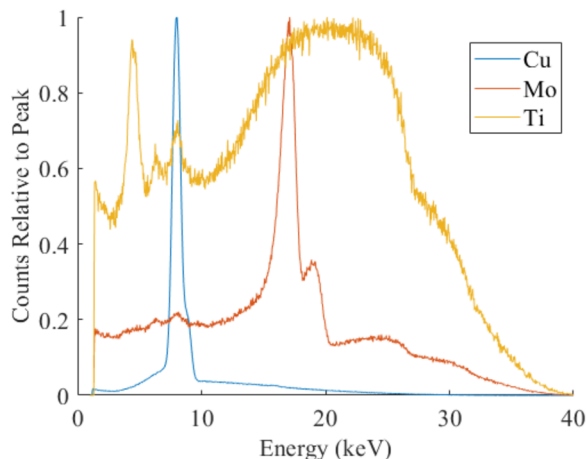
FIG. 3. Unfiltered spectra for the three anode tubes used in the Proto-XRD source.

B. Characterizing known filters

In order to benchmark the system, measurement of x-ray transmission curves for a set of extremely pure, x-ray quality aluminum filters was undertaken. For these measurements, the copper x-ray anode tube was utilized. A representative dataset from this process taken for a filter with an areal density (related to the filter thickness by a factor of the density of pure aluminum) of 34.6 mg/cm^2 (corresponding to a thickness of 128.15 μm—assuming a perfect solid aluminum density in our sample, which was manufactured with x-ray quality filtration in mind) is shown in Figs. 4 and 5.

After normalizing the spectra, the transmission curve $\Theta(E)$ was calculated and a nonlinear regression (based on tabulated data of x-ray transmission[6]) was used to fit a thickness of aluminum to
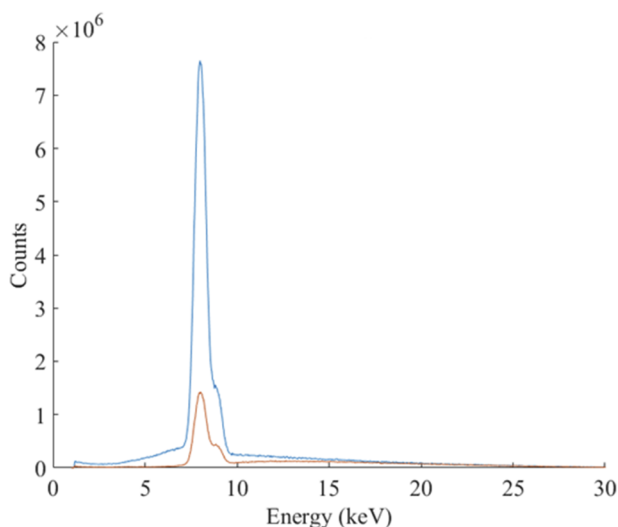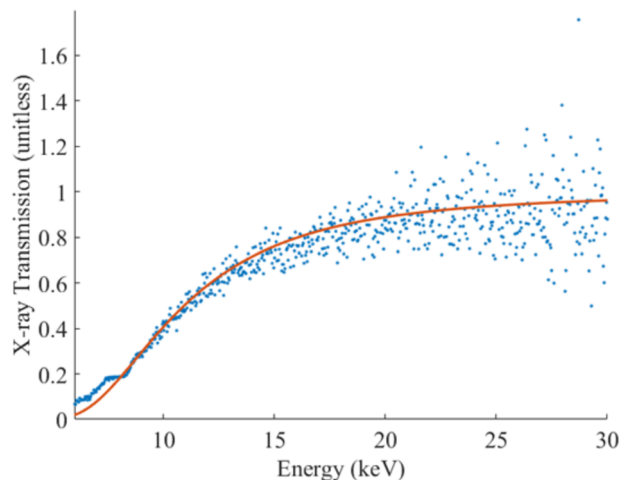

FIG. 5. Calculated transmission data (blue) from the spectra shown in Fig. 4 plotted together with a fit obtained via nonlinear regression (orange) over an energy range of 5–15 keV. The filter areal density calculated from this regression is 34.21 ± 0.6750 mg/cm^2.

the observed transmission curve. In the data shown in Figs. 4 and 5, the actual transmission characteristics of the filter are accurately captured by our regression procedure—with a filter areal density of 34.6 mg/cm^2, an areal density of 34.21 ± 0.6750 mg/cm^2 was computed. This good characterization was repeatable for the other filters in the dataset; a plot of the difference between the calculated areal densities using the x-ray test bench and the actual areal densities for aluminum filters with varying areal density is shown in Fig. 6. Because we are able to reproduce the known values for these filters to within statistical uncertainty, we conclude that the x-ray test bench
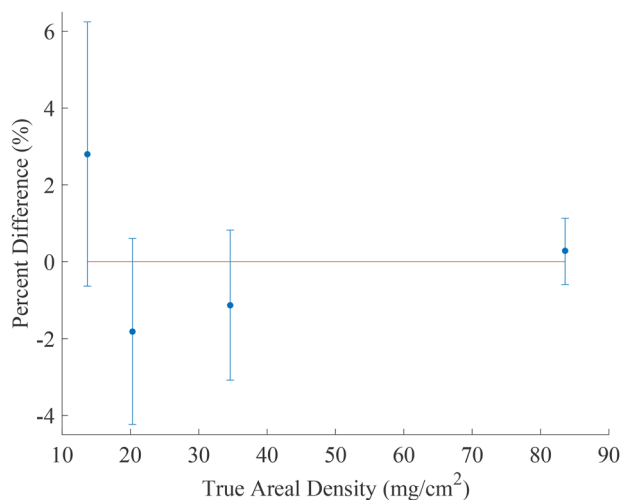

FIG. 4. Normalized filtered and unfiltered spectra for an aluminum filter with a known areal density of 34.6 mg/cm^2. The unfiltered spectrum is plotted in blue, while the filtered spectrum is plotted in orange.

FIG. 6. The percent difference between the calculated value of filter areal density and the true areal density for each filter plotted against the true areal density. The error bars here are statistical and represent a 95% confidence interval on the fitted value.

is capable of accurately measuring the x-ray transmission curves of these filters. We also note that using a smaller fit range, centered around the high-intensity copper peak, does not result in significantly different inferred thicknesses (the results are within the error bars presented in this report).

C. Measuring unknown filters

Having confirmed the consistency of the x-ray test bench, the setup was used to characterize the transmission curves of filters whose x-ray transmission properties were not initially known and to compare them to x-ray transmission that one might expect from the physical thickness of a nominal density pure filter.

1. Aluminum

The first set of unknown filters that were characterized were aluminum filters with nominal thicknesses of 100, 200, or 300 μm. The results of these measurements are shown in Fig. 7.

It can be seen immediately that our calculated values do not match the nominal physical thickness for any of the three; instead, it is inferred that these filters have lower transmission (and thus higher inferred thicknesses) than that would be suggested by the nominal values. It is possible that this effect is due to some high-Z contaminant, which can dramatically affect the shape of the transmission curve and thus the value fitted by our regression procedure, which assumes a pure sample (Fig. 8 shows the difference between the measured and inferred transmission curves). Additionally, because absorption is fundamentally an exponential function of areal density, slight variations in the thickness of the filter can have unexpectedly large effects on the filter's absorption properties. Such thickness variations could also account for the mismatch between nominal and calculated values.

2. Titanium

The second set of unknown filters characterized was titanium filters with nominal thicknesses of 100, 200, or 500 μm. These

FIG. 8. A sample transmission curve calculated from the 100 μm aluminum filter. The experimentally obtained data are shown in blue, with the inferred fit shown in orange.

samples were characterized using the molybdenum anode. The results of this study are shown in Fig. 9.

Once again, note that for filters that are not specifically designed to be of x-ray quality, the thicknesses of the filters inferred from the x-ray transmission curve do not match the nominal physical thickness. However, for these titanium filters, the deviations from equality are smaller than those in the aluminum filters discussed in Sec. IV C 1 and the deviations are not consistently directed—both higher and lower inferred thicknesses are observed.
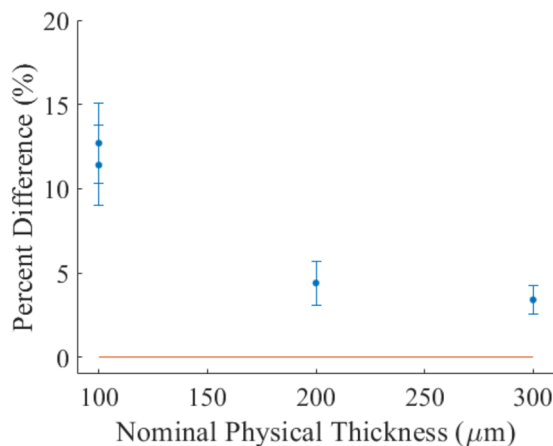

FIG. 7. The percent difference between the calculated value of filter thickness and the nominal physical thickness for each filter plotted against the nominal thickness. The error bars here are statistical and represent a 95% confidence interval on the fitted value. Long exposure times have resulted in high statistics and relatively small error bars.
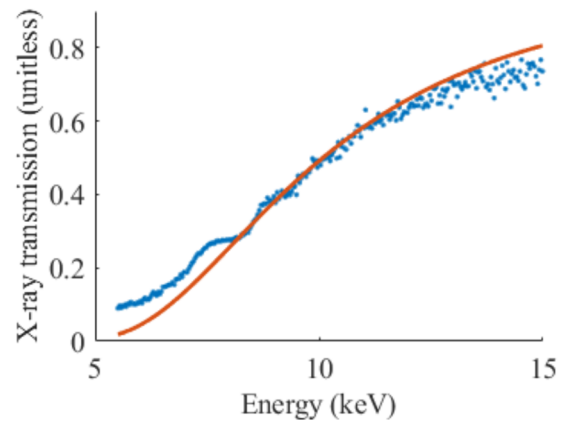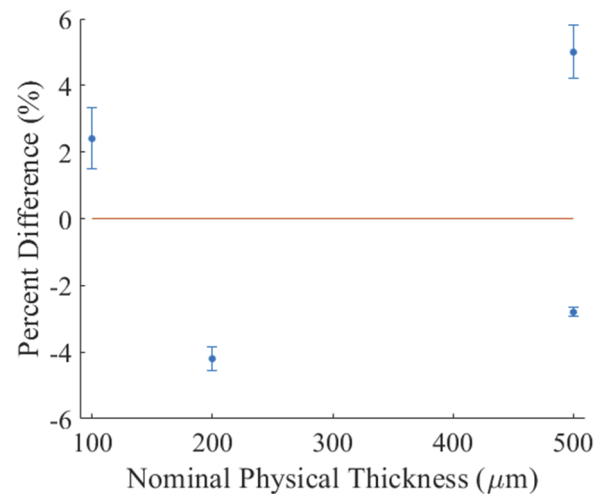

FIG. 9. The percent difference between the calculated value of filter thickness and the nominal physical thickness for each filter plotted against the nominal thickness. The orange line represents equality between the two values. The error bars here are statistical and represent a 95% confidence interval on the fitted value. Long exposure times have resulted in high statistics and relatively small error bars.

V. CONCLUSIONS AND PATH FORWARD

By using a partially depleted surface barrier detector together with an AMPTEK 123-CdTe x-ray spectrometer and a custom Proto-XRD source, we have developed an x-ray test bench facility, which is able to accurately measure both the energy spectrum and time-resolved x-ray fluence of the source. By measuring these quantities, energy-dependent x-ray transmission curves $\Theta(E)$ for a variety of different filters have been measured. Measurements made with the test bench were able to reproduce the known thicknesses of x-ray quality aluminum filters to within uncertainty bounds across an order of magnitude of areal densities. The quality of these measurements validates the transmission measurements made for previously uncharacterized aluminum and titanium filters. These measurements are more accurate characterizations of the filters' x-ray transmission properties than their nominal thicknesses and suggest that measurements similar to these should be performed for filters used in x-ray diagnostics across the HEDP field.

DATA AVAILABILITY

The data that support the findings of this study are available from the corresponding author upon reasonable request.

REFERENCES

[1] N. Kabadi, A. Sorce, C. Stoeckl, H. W. Sio, P. Adrian, M. Bedzyk, J. Frenje, J. Katz, J. Knauer, J. Pearcy, D. Weiner, B. A. Aguirre, R. Betti, A. Birkel, D. Cao, M. Gatu-Johnson, D. Patel, R. D. Petrasso, and S. P. Regan, "A multi-channel x-ray temporal diagnostic for measurement of time-resolved electron temperature in cryogenic deuterium-tritium implosions at OMEGA," Rev. Sci. Instrum. **92**, 023507 (2021).

[2] P. Adrian, J. Frenje, B. Aguirre, B. Bachmann, A. Birkel, M. Gatu-Johnson, N. V. Kabadi, B. Lahmann, C. K. Li, O. M. Mannion, W. Martin, Z. L. Mohamed, S. P. Regan, H. G. Rinderknecht, B. Scheiner, M. J. Schmitt, F. H. Seguin, R. C. Shah, H. Sio, C. Sorce, G. D. Sutcliffe, and R. D. Petrasso, "An x-ray penumbral imager for measurements of electron -temperature profiles in inertial confinement fusion implosions at OMEGA," Rev. Sci. Instrum. **92**, 043548 (2021).

[3] B. L. Henke, H. T. Yamada, and T. J. Tanaka, "Pulsed plasma source spectrometry in the 80-8000 eV x-ray region," Rev. Sci. Instrum. **54**, 1311 (1983).

[4] L. C. Jarrott, L. R. Benedetti, H. Chen, N. Izumi, S. F. Khan, T. Ma, S. R. Nagel, O. L. Landen, A. Pak, P. K. Patel, M. Schneider, and H. A. Scott, "Hotspot electron temperature from x-ray continuum measurements on the NIF," Rev. Sci. Instrum. **87**, 11E534 (2016).

[5] S. F. Khan, P. M. Bell, D. K. Bradley, S. R. Burns, J. R. Celeste, L. S. Dauffy, M. J. Eckart, M. A. Gerhard, C. Hagmann, D. I. Headley, J. P. Holder, N. Izumi, M. C. Jones, J. W. Kellogg, H. Y. Khater, J. R. Kimbrough, A. G. Macphee, Y. P. Opachich, N. E. Palmer, R. B. Petre, J. L. Porter, R. T. Shelton, T. L. Thomas, and J. B. Worden, "Measuring x-ray burn history with the Streaked Polar Instrumentation for Diagnosing Energetic Radiation (SPIDER) at the National Ignition Facility (NIF)," Proc. SPIE **8505**, 850505 (2012).

[6] S. Seltzer, Tables of X-Ray Mass Attenuation Coefficients and Mass Energy-Absorption Coefficients, NIST Standard Reference Database 126, 1995, type: dataset.

[7] Amptek, X-123cdte complete x-ray and gamma ray spectrometer.

[8] Ortec, Silicon charged particle radiation detectors.